CDK1 Inhibition Targets the p53-NOXA-MCL1 Axis, Selectively Kills Embryonic Stem Cells, and Prevents Teratoma Formation

Noelle E. Huskey,[1] Tingxia Guo,[3] Kimberley J. Evason,[1,2] Olga Momcilovic,[1] David Pardo,[1] Katelyn J. Creasman,[1] Robert L. Judson,[4,5] Robert Blelloch,[4,5] Scott A. Oakes,[2,6] Matthias Hebrok,[3] and Andrei Goga[1,6,*]

[1]Department of Cell and Tissue Biology and Medicine
[2]Department of Pathology
[3]Diabetes Center
[4]Eli and Edythe Broad Center of Regeneration Medicine and Stem Cell Research
[5]Department of Urology
[6]Helen Diller Family Comprehensive Cancer Center
University of California, San Francisco, San Francisco, CA 94143, USA
*Correspondence: andrei.goga@ucsf.edu
http://dx.doi.org/10.1016/j.stemcr.2015.01.019

SUMMARY

Embryonic stem cells (ESCs) have adopted an accelerated cell-cycle program with shortened gap phases and precocious expression of cell-cycle regulatory proteins, including cyclins and cyclin-dependent kinases (CDKs). We examined the effect of CDK inhibition on the pathways regulating proliferation and survival of ESCs. We found that inhibiting cyclin-dependent kinase 1 (CDK1) leads to activation of the DNA damage response, nuclear p53 stabilization, activation of a subset of p53 target genes including NOXA, and negative regulation of the anti-apoptotic protein MCL1 in human and mouse ESCs, but not differentiated cells. We demonstrate that MCL1 is highly expressed in ESCs and loss of MCL1 leads to ESC death. Finally, we show that clinically relevant CDK1 inhibitors prevent formation of ESC-derived tumors and induce necrosis in established ESC-derived tumors. Our data demonstrate that ES cells are uniquely sensitive to CDK1 inhibition via a p53/NOXA/MCL1 pathway.

INTRODUCTION

Embryonic stem cells (ESCs) are derived from the inner cell mass of the blastocyst, during a stage of development defined by rapid cell division rates. Mouse and human ESCs grown in culture retain the rapid proliferation observed in early embryonic cells, exhibiting an accelerated cell-cycle program characterized by a shortened G1 phase and differentially regulated cell-cycle checkpoints (Orford and Scadden, 2008). When ESCs differentiate, their cell-cycle structure changes to incorporate a longer G1 phase and slower proliferation rates. Whether their unique cell-cycle program alters ESC dependency on cell-cycle regulatory proteins has not been previously established.

Cell-cycle adaptations that account for the altered ESC cell-cycle structure were first identified in mouse ESCs (mESCs) (Ballabeni et al., 2011; Orford and Scadden, 2008). Cyclin/CDK complexes represent the key enzymes that regulate orderly progression through the mammalian cell cycle. In somatic cells, cyclin abundance fluctuates throughout the cell cycle, in part due to degradation by the anaphase-promoting complex/cyclosome (APC/C) at the end of mitosis (reviewed in Morgan, 2007). In mESCs, however, APC/C activity is attenuated due to high levels of EMI1 (early mitotic inhibitor 1), resulting in reduced fluctuation of cyclin expression (Ballabeni et al., 2011).

Additionally, mESCs express higher levels of cyclins E, A, and B compared to somatic cells (Stead et al., 2002) and do not appreciably express the endogenous CDK inhibitors, including INK family members (p15, p16, and p19) and CIP/KIP family members (p21 and p27) (Sabapathy et al., 1997).

Cell-cycle adaptations in human ESCs (hESCs) are less defined. In contrast to mESCs, hESCs exhibit significant fluctuation of cyclin expression in a cell-cycle-dependent manner (Neganova et al., 2009), indicating differences in the regulation of key cell-cycle proteins between the two cell types. Similar to mESCs however, hESCs exhibit high expression of cyclins A and E as well as undetectable expression of p21 and p27 (Becker et al., 2006). In both cell types, elevated cyclin activity combined with lack of endogenous CDK inhibitors results in increased activity of CDK1 and 2 and diminished G1 and G2 cell-cycle phases.

It remains unknown if the altered cell-cycle program employed by mouse and human ESCs results in unique dependencies on individual cell-cycle proteins. Furthermore, whether there is a connection between the ES cell-cycle program and the cell-death pathways employed by ESCs has not been explored. Acute inhibition of CDK1 or CDK2 in proliferating somatic cells generally results in reversible arrest of the cell cycle without significant cell death (Gray et al., 1998; Horiuchi et al., 2012;

CrossMark

van den Heuvel and Harlow, 1993). Here, we use small interfering RNA (siRNA) knockdown and small molecule CDK inhibitors to identify critical pathways regulating cell proliferation and survival in mouse and human ESCs.

RESULTS

Depletion of CDK1, Cyclin A, or Cyclins B1/B2 Causes Apoptosis in Mouse Embryonic Stem Cells

To determine if mESCs exhibit unique dependencies on cell-cycle regulatory proteins, we transiently transfected small interfering RNAs (siRNAs) to systematically deplete CDKs 1 and 2, and cyclins D, E1/E2, A2, and B1/B2. 72 hr post-transfection, western blot analysis revealed effective and specific siRNA-mediated knockdown of these proteins (Figure 1A).

We evaluated the effects of CDK/cyclin knockdown on the mES cell cycle using propidium iodide (PI) to stain for DNA content. Knockdown of CDK2, cyclin D, or cyclins E1/E2 had little effect on cell-cycle profiles (Figure 1B), consistent with existing reports in somatic cells and mouse knockout models (Barrière et al., 2007; Li et al., 2012; Tetsu and McCormick, 2003) and did not significantly affect mESC viability, as measured using sub-2N DNA content as a marker of cell fragmentation and death (Figures 1B and 1C). Western blotting showed no evidence of poly (ADP-ribose) polymerase (PARP) cleavage, a marker of caspase-dependent apoptosis (Figure 1D), and microscopic evaluation of mESC morphology (Figure 1B) revealed findings consistent with viable cells.

In contrast, knockdown of cyclin A resulted in an increased percentage of live cells in the S and G2/M phases, and a reduced percentage of live cells in G1 (Figure 1B). This is similar to findings reported in cyclin-A-deficient ES cells (Kalaszczynska et al., 2009). Knockdown of cyclin A also resulted in an approximate 20% increase in the percentage of fragmented cells (Figure 1C) and a small increase in PARP cleavage (Figure 1D), compared to control siRNA. Knockdown of CDK1, or cyclins B1/B2, resulted in more pronounced cell fragmentation (approximately 30% and 55%, respectively) (Figures 1B and 1C) and PARP cleavage (Figure 1D). Thus, depletion of CDK1 or its cyclin binding partners (cyclins A2 and B1/B2)—but not other CDKs and cyclins—induces cell death in mESCs.

Previous reports have shown that CDK1 inhibition induces differentiation in some types of pluripotent cells (Ullah et al., 2008). We found no evidence of differentiation of mESCs after siRNA-mediated knockdown of any of the CDKs or cyclins (Figure S1). This is consistent with findings that elongation of the mES cell cycle is compatible with pluripotency (Li et al., 2012).

Small-Molecule-Mediated Inhibition of CDK1 Induces Apoptosis in mESCs

A more clinically relevant method to disrupt CDK activity involves small molecule inhibitors that block kinase activity at the ATP-binding site. We asked if small molecule inhibition of CDK1 would result in similar effects as those seen after siRNA-mediated knockdown. mESCs were treated with a CDK2 inhibitor, CVT-313 (5 μM), and two CDK1 inhibitors, purvalanol A (10 μM) and Ro-3306 (9 μM). Inhibitors were used at concentrations shown to effectively target the activity of the kinases in prior studies (Brooks et al., 1997; Goga et al., 2007; Gray et al., 1998; Vassilev et al., 2006). Similar to CDK2 knockdown, treatment with CDK2 inhibitor CVT-313 had no effect on sub2n DNA content (Figures 2A and 2B). In contrast, CDK1 inhibitors purvalanol A and Ro-3306 caused cell-cycle arrest at G2/M and significant sub-2n levels (approximately 45% and 35%, respectively, compared to a DMSO-treated control) within 24 hr of treatment (Figures 2A and 2B). As purvalanol A produced a stronger effect than Ro-3306 treatment, we exclusively used purvalanol A in subsequent experiments. Thus, similar to siRNA mediated CDK1 and cyclin B knockdown, small molecule inhibitors of CDK1 elicit cell death in mESCs.

Differentiated mESCs Are Resistant to CDK1 Inhibition

We induced mESCs to differentiate by removing leukemia inhibitory factor (LIF) from the media and adding a low dose of all-*trans* retinoic acid (RA). After 4 days of RA treatment, mRNA levels of the pluripotency marker, *Oct4*, were reduced over 100-fold (Figure S2A). Additionally, OCT4 and a second pluripotency marker, Nanog, showed a markedly reduced expression by immunofluorescence (Figure S2B). Cell-cycle analysis of differentiated mES cells (mES-diff) showed that 46% of cells were in S or G2/M phases (28% in S and 18% in G2/M) indicating that these cells are actively proliferating (Figure 2C). mES-diff cells treated with purvalanol A underwent a G2/M arrest, suggesting that CDK1 was being targeted and the cells were actively cycling prior to the G2/M block (Figure 2C). In contrast to undifferentiated cells, mES-diff cells did not undergo cell death (Figure 2C). To confirm these results, we assessed levels of apoptosis using a nucleic acid dye exclusion viability assay and western blotting for PARP cleavage to compare the effect of purvalanol A treatment on mES-diff cells and a second differentiated cell type, mouse embryonic fibroblasts (MEFs), with mESCs and mouse-induced pluripotent stem cells (miPSCs). mESCs and miPSCs underwent apoptosis, while the differentiated cell types did not (Figures 2D and 2E). We generated dose-response curves, using percentage cell death as a response, and found that the relative half-maximal response (EC$_{50}$) values for
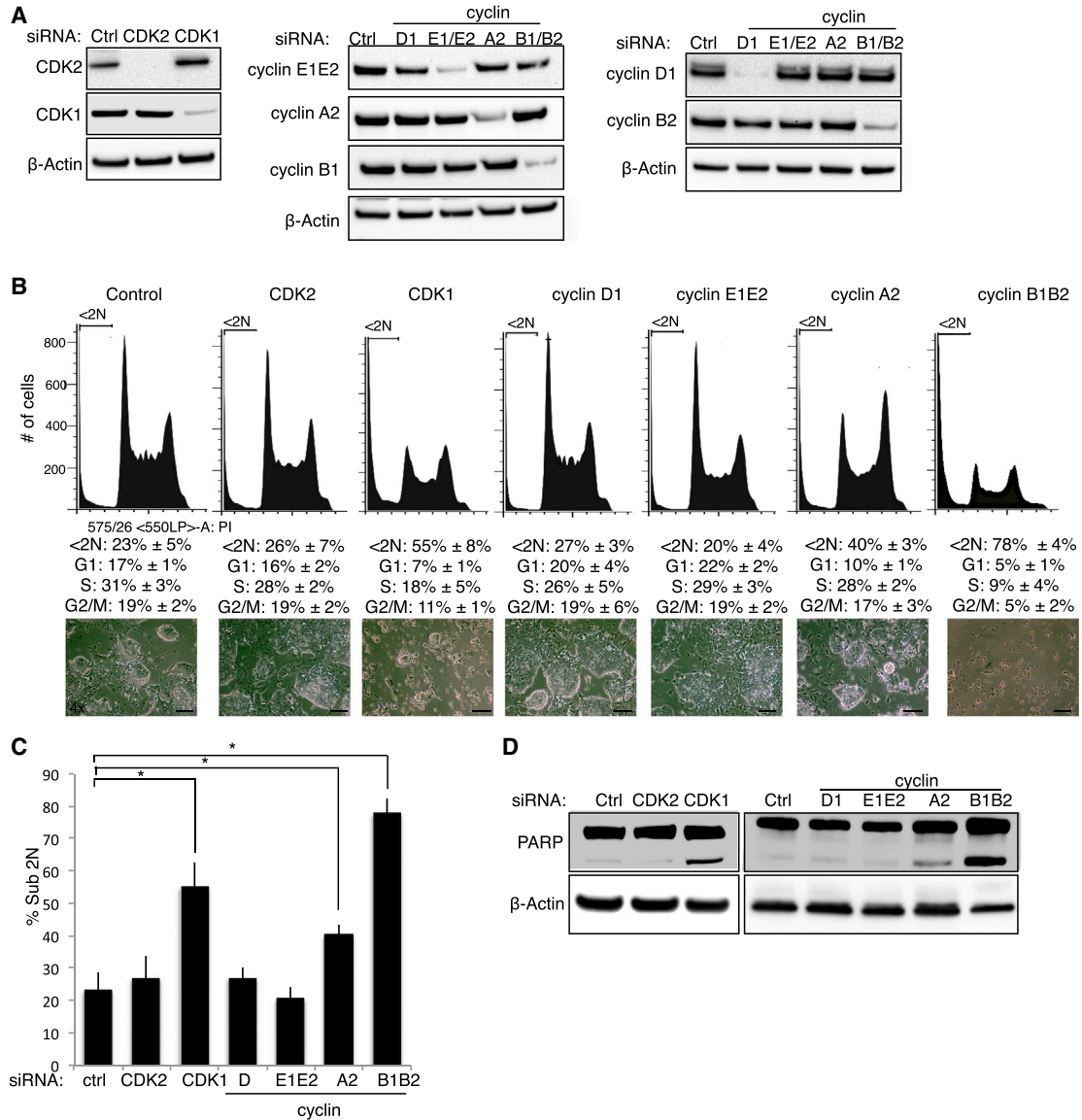
Figure 1. siRNA Knockdown of CDK1 and CDK1 Cyclin Binding Partners Induces Apoptosis in mESCs
(A) Western blots of CDKs and cyclins protein levels 72 hr after siRNA transfection in mESCs. Ctrl, non-targeting control siRNA.
(B) Cell-cycle distribution 72 hr after siRNA transfection. Percentage of cells in each cell-cycle phase is indicated (mean ± SEM, n = 3 independent experiments). Morphology of cells after siRNA knockdown. Scale bars, 140 μm.
(C) sub2N DNA content from (B) (mean ± SEM, n = 3). Populations compared using Student's t test, *p < 0.03.
(D) PARP cleavage by western blotting.
See also Figure S1.

purvalanol A treatment against mES and mES-diff cells differed significantly (Figure 2F). Collectively, these data demonstrate that CDK1 inhibition selectively induces cell death in pluripotent cells while sparing differentiated cells.

The determine if the difference in sensitivity to CDK1 inhibitors was due to the difference in proliferation rates between mESC and differentiated cells, we employed mESCs that are deficient for DGCR8, which is essential for miRNA biogenesis (Wang et al., 2007). $Dgcr8^{-/-}$ mESCs proliferate slower, with a lengthened G1 phase compared to wild-type mESCs, exhibiting a cell-cycle program similar to that of somatic cells (Wang et al., 2007). Despite a lower proliferative index, $Dgcr8^{-/-}$ mESCs underwent similar levels of cell death as wild-type (WT) mESCs after CDK1 inhibitor treatment (Figure 2D), suggesting that a difference in cell-cycle dependency and/or cell-death pathways, rather
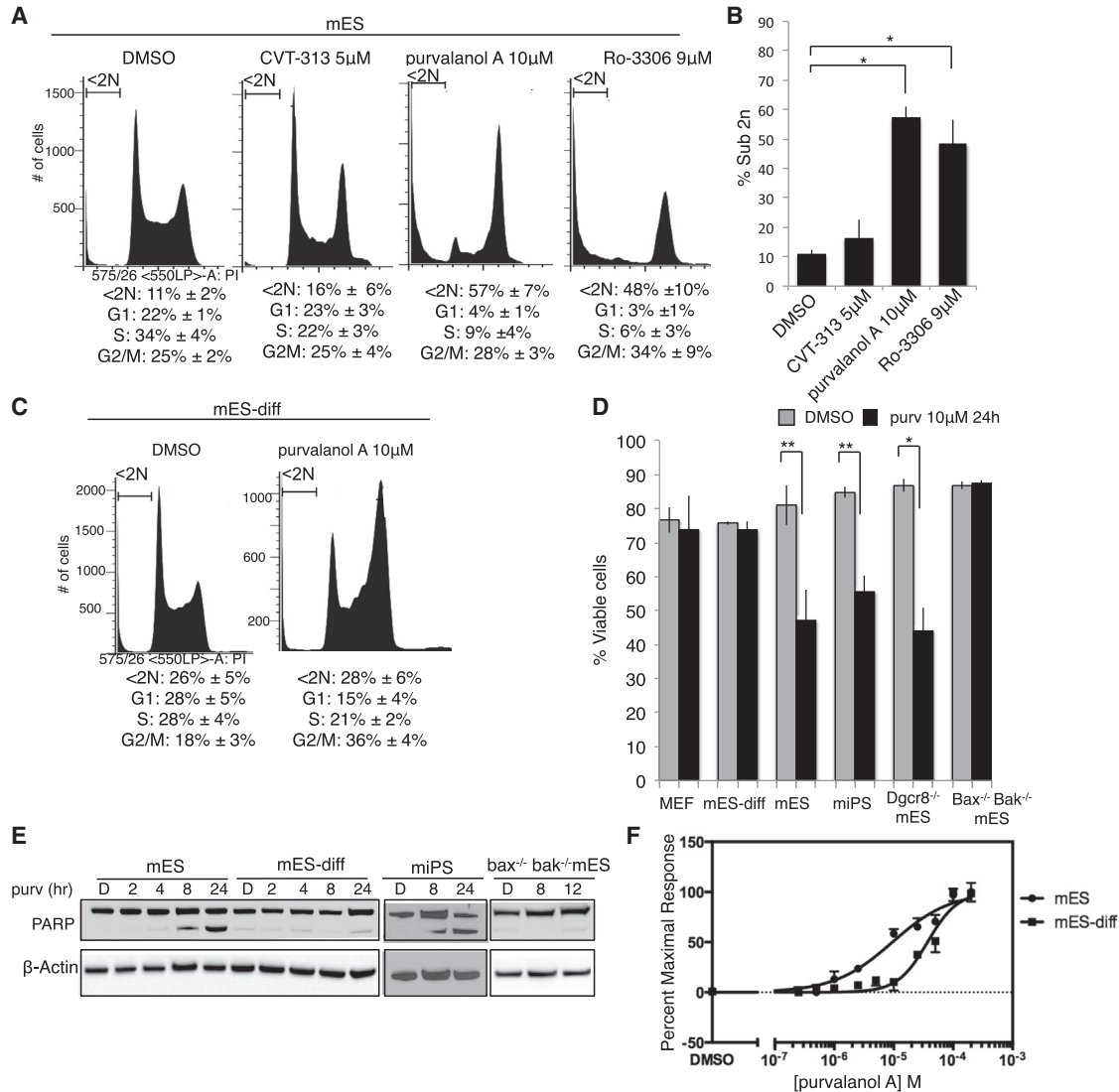
Figure 2. Small Molecule Inhibition of CDK1 Kills mESCs but Not Differentiated Cells

(A) Effect of CDK inhibitors on mES cell-cycle distribution. Percentage of cells in each cell-cycle phase (mean ± SEM, n = three independent experiments).

(B) sub2N DNA content from (A) (mean ± SEM, n = three independent experiments). Populations were compared using Student's t test, *p < 0.006.

(C) Effect of CDK inhibitors on differentiated mES (mES-diff) cell-cycle distribution. Percentage of cells in each cell-cycle phase (mean ± SEM, n = 3 independent experiments).

(D) Cell viability after 24-hr treatment with DMSO or purvalanol A (purv) (10 μM), (mean ± SEM, n > 4 independent experiments). Populations compared using a Student's t test, **p < 0.005, *p = 0.018.

(E) Western blot for PARP cleavage after purvalanol A (purv) treatment for indicated times in hours; D, DMSO control.

(F) Dose-response curve for purvalanol A treatment of mES and mES-diff cells to determine (EC_{50}) for each cell type (9.48 μM mES and 36.9 μM mES-Diff). Response measured as percentage maximum cell death for each cell type. p < 0.0001, determined by Fisher's exact test. See also Figure S2.

then proliferation rates, contribute to the unique CDK1-inhibitor-induced cell death observed in pluripotent cells.

To identify cell-death pathways involved in CDK1-inhibitor-induced cell death, we utilized mES cells deficient in the pro-apoptotic proteins, BCL2 homologous antagonist killer (BAK) and Bcl2-associated protein X (BAX), two proteins that are required for the intrinsic (mitochondrial) apoptotic pathway (Wei et al., 2001). $Bax^{-/-}Bak^{-/-}$ mESCs

were derived from previously described mice with a germline deletion of *Bak* and a conditional allele of *Bax*$^{Flox/-}$, followed by deletion of the *Bax* allele with Cre-recombinase (E.S. Wang, N.A. Reyes, C. Melton, N.E.H., A.G., R.B., and S.A.O., unpublished data) (Takeuchi et al., 2005). These cells maintain expression of OCT4 and Nanog (Figure S2B) but lack expression of BAX and BAK (Figure S2C). *Bax*$^{-/-}$ *Bak*$^{-/-}$ mESCs treated with purvalanol A underwent a G2/M arrest, suggesting that purvalanol A effectively targets CDK1 in these cells (Figure S2D). In contrast to WT mESCs, treatment of *Bax*$^{-/-}$*Bak*$^{-/-}$ mESCs with purvalanol A induced no cell death (Figure 2D) or PARP cleavage (Figure 2E). These data indicate that CDK1-inhibitor-induced cell death in pluripotent cells occurs via the intrinsic apoptotic pathway.

CDK1 Inhibitor Treatment Induces a DNA Damage Response in Mouse ES, but Not Differentiated, Cells

CDKs regulate several components of the DNA damage response pathway, and CDK1 activity is critical for repair of double-stranded breaks (DSB) by homologous recombination (HR) (Falck et al., 2012; Johnson et al., 2011; Peterson et al., 2011). Additionally, it has been shown that ESCs are highly sensitive to DNA damage, more frequently undergoing apoptosis relative to differentiated cells (Liu et al., 2013; Momcilovic et al., 2010). We hypothesized that CDK1 inhibition triggers the DNA damage response in mESCs. To address this hypothesis, we examined the effect of CDK1 inhibition on the phosphorylation of H2AX in WT mES, *Bax*$^{-/-}$ *Bak*$^{-/-}$ mES, and mES-diff cells. Phosphorylation of H2AX at S139 (γ-H2AX) occurs as an early cellular response to DNA damage in mammalian cells. As a positive control, cells were treated with doxorubicin, a topoisomerase II inhibitor known to cause DSBs. Treatment of WT and *Bax*$^{-/-}$ *Bak*$^{-/-}$ mESCs with purvalanol A resulted in an increase in γ-H2AX levels, comparable to treatment with doxorubicin (Figure 3A). Because *Bax*$^{-/-}$ *Bak*$^{-/-}$ mESCs do not undergo CDK-inhibitor-induced cell death, they are useful for identifying cellular effects occurring upstream of cell death. Thus, our data suggest that CDK1 inhibition induces a DNA damage response upstream of apoptosis in mESCs. Purvalanol A did not increase γ-H2AX levels in mES-diff cells, indicating that CDK-inhibition-induced activation of the DNA damage response is unique to pluripotent cells (Figure 3A). Consistent with our western blot results, we observed an increase in the percentage of *Bax*$^{-/-}$ *Bak*$^{-/-}$ mESCs—but not differentiated mESCs—containing γ-H2AX foci after treatment with purvalanol A, by immunofluorescence (Figure 3B). Additionally, we saw an increase in levels of phosphorylated ATM (S1981), a marker of DSBs (Shiloh, 2003), in *Bax*$^{-/-}$ *Bak*$^{-/-}$ ESCs, but not mES-diff cells, after purvalanol A treatment (Figure 3C). These data indicate that CDK1 inhibition acti-vates the DNA damage response pathway in mES, but not differentiated, cells.

CDK1-Inhibitor-Induced Cell Death in mES Cells Is Mediated by p53

In response to DNA damage, the p53 tumor suppressor protein initiates transcription of numerous target genes involved in cell-cycle arrest and apoptosis (Vousden and Lu, 2002). We asked if p53 mediates CDK1-inhibitor-induced cell death in mESCs. Upon treatment with purvalanol A, mESCs deficient for p53 (Sabapathy et al., 1997) underwent a G2/M arrest, indicating that CDK1 was effectively inhibited (Figure 4A). Cell viability assays, however, revealed that *p53*$^{-/-}$ mESCs were significantly less sensitive to CDK1 inhibition relative to WT mESCs, with nearly 80% of *p53*$^{-/-}$ mESCs versus 40% of WT mESCs remaining viable after treatment with purvalanol A (Figure 4B). Consistent with this finding, western blot analysis revealed PARP cleavage in WT, but not p53-deficient, mESCs (Figure 4C), suggesting that p53 mediates CDK1-inhibitor-induced cell death in mESCs.

p53 activity is regulated at multiple levels, including protein stability and subcellular localization. Phosphorylation of serine 18 (serine 15 in human) of p53 by ATM during the DNA damage response inhibits degradation of p53, thus increasing p53 stability (Canman et al., 1998). We examined total p53 protein and phospho-serine 18 (S18) levels after CDK inhibitor treatment in WT mESCs, *Bax*$^{-/-}$ *Bak*$^{-/-}$ mESCs, and mES-diff cells, using doxorubicin-treated cells as a positive control. Purvalanol A treatment increased p53 levels in WT mESCs and *Bax*$^{-/-}$ *Bak*$^{-/-}$ mESCs within 4 hr of treatment, comparable to treatment with doxorubicin, which was accompanied by phosphorylation of S18 (Figure 4D). The levels of total and phosphorylated p53 in mES-diff cells did not increase after purvalanol A treatment (Figure 4D), indicating that induction of p53 protein levels after CDK1 inhibition is unique to mESCs. We observed a similar increase in p53 levels after siRNA knockdown of CDK1 and cyclins A or B1 and B2 in mESCs, but not siRNA knockdown of cyclins D, E1/E2, or CDK2 (Figure 4E), suggesting that induction of p53 is due to CDK1 inhibition rather then an off-target effect of purvalanol A.

Phosphorylation of S18 by ATM inhibits the nuclear export of p53 by masking a nuclear export signal (Zhang and Xiong, 2001). To determine the localization of p53 in mESCs after CDK1 inhibitor treatment, we isolated cytosolic and nuclear fractions and analyzed p53 protein expression via western blot. Purvalanol A induced localization of p53 within the nuclear fraction of mESCs (Figure 4F). These data indicate that p53 is stabilized in the nucleus in response to CDK1 inhibitor treatment in mESCs.
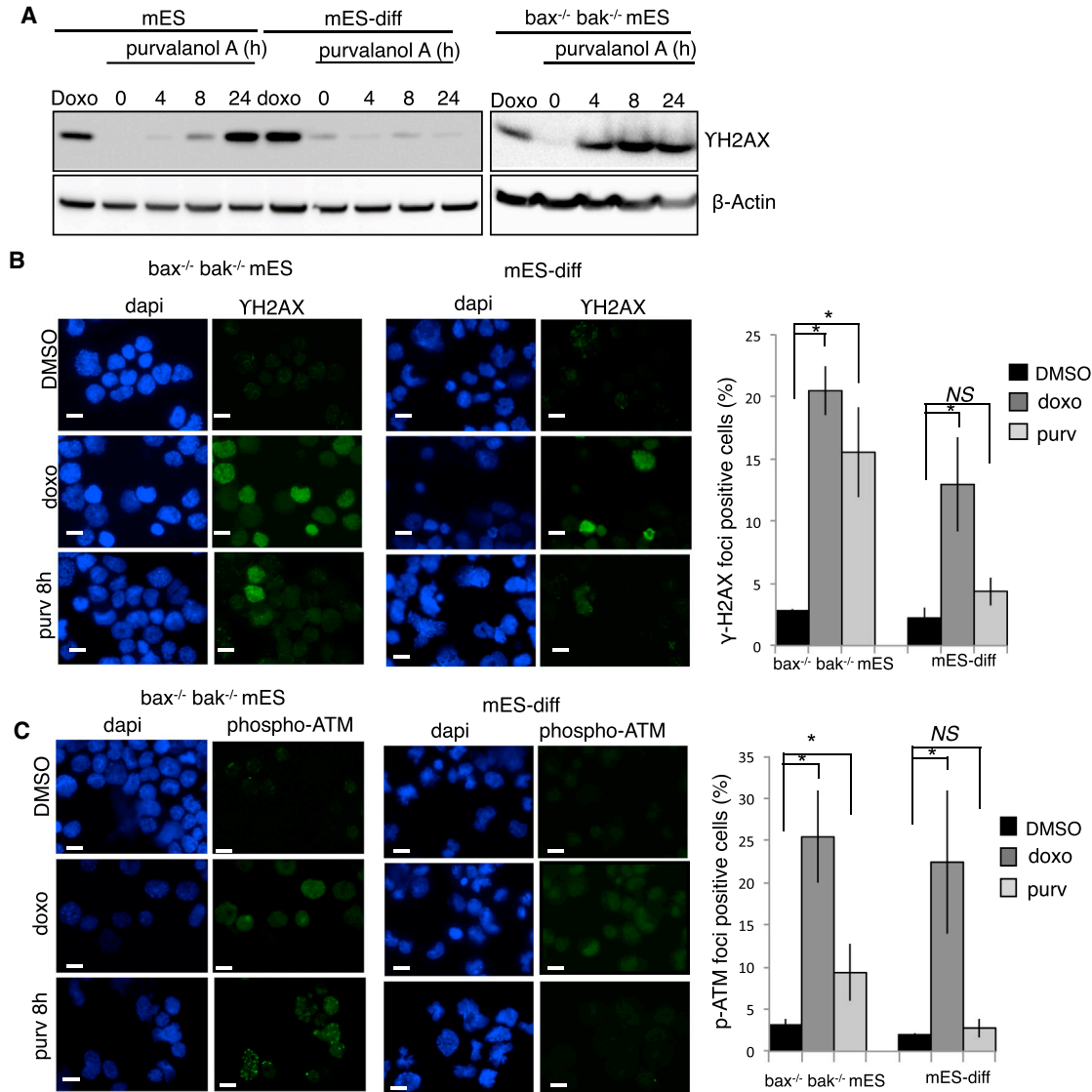
Figure 3. Inhibition of CDK1 Induces the DNA Damage Response in ES but Not Differentiated Cells
(A) Western blot for γ-H2AX.
(B and C) Detection of γ-H2AX foci (B) or phosphorylated ATM (S1981) (pATM) (C) by immunofluorescence in $Bax^{-/-}Bak^{-/-}$ mESCs and differentiated mES (mES-diff). DAPI (blue) indicates cell nuclei. Cells were treated with DMSO as a negative control, 1 μM doxorubicin (doxo) as a positive control, or 10 μM purvalanol A (purv) for 8 hr. Scale bars, 20 μm. Histograms represent mean ± SEM percentage of cells expressing γ-H2AX foci (B) or pATM (C), n = 4 independent experiments. Populations compared using a Student's t test *p < 0.05; NS, not significant.

CDK1 Inhibition Induces Expression of BCL2 Family Member NOXA and Depletes MCL1 to Induce Cell Death in mESCs

To identify the pathways that are activated downstream of p53 after CDK1 inhibitor treatment, we used a quantitative PCR-based array to examine mRNA expression levels of p53 transcriptional targets in mES and mES-diff cells, after 8 hr of purvalanol A treatment. At 8 hr, p53 activation occurs (Figure 4D), but minimal cell death, as measured by PARP

cleavage, is observed (Figure 4C). Surprisingly, many p53 transcriptional targets involved in apoptosis—including *Bax* and *Bbc3* (PUMA)—were not significantly altered upon purvalanol A treatment of mESCs (Figure 5A). However, we did observe a significant increase in four established p53 targets, *Pmaip1 (*NOXA), *Rb, Trp73 (*TP73), and *Zmat3* (WIG1) (Figure 5A). Consistent with our observations that p53 activity is not induced in mES-diff cells following CDK1 inhibitor treatment, we did not observe
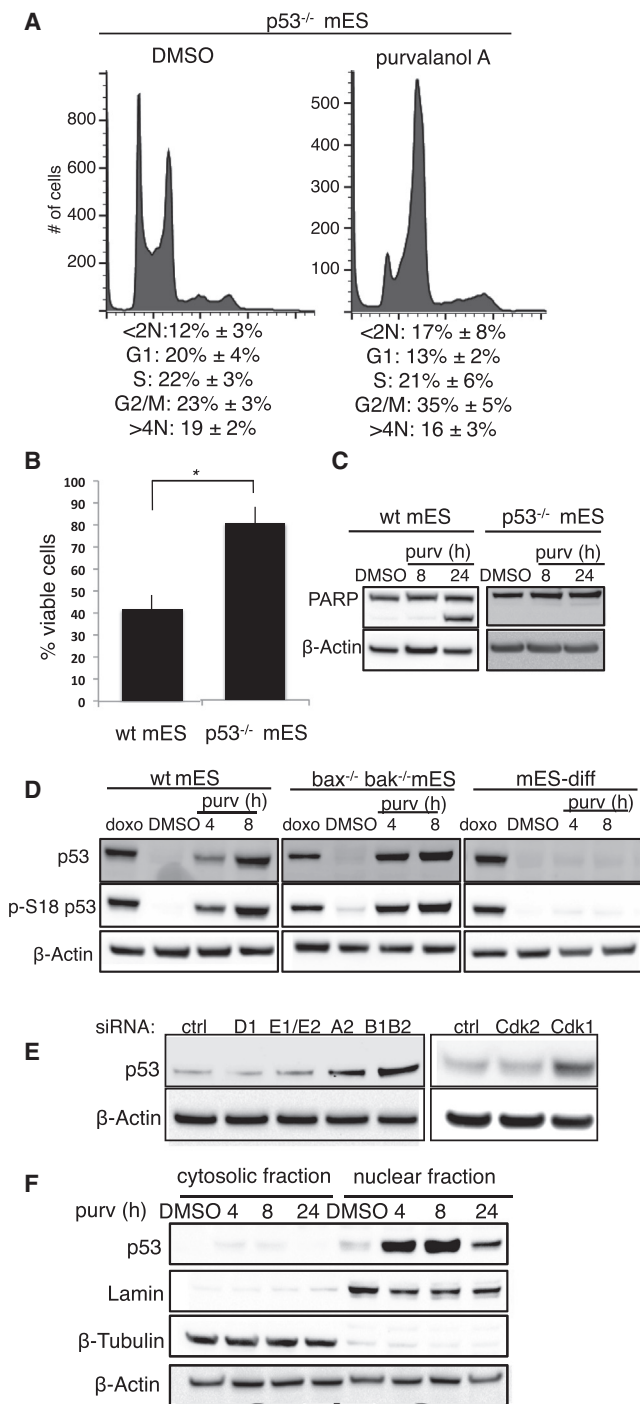
Figure 4. CDK1-Inhibitor-Induced Cell Death in mESCs Is Mediated by p53

(A) Effect of purvalanol A on $p53^{-/-}$ mESC cycle distribution. Percentages of cells in each cell-cycle phase (mean ± SEM, n = 3 independent experiments).

(B) Cell viability after 24 hr of treatment, 10 μM purvalanol A, normalized to DMSO-treated controls (mean ± SEM n = 5 independent experiments). Populations compared using a Student's t test *p = 0.004.

(C) PARP cleavage after purvalanol A (purv) treatment for the indicated amount of hours (h) shown by western blot.

(D) Western blot for p53, and phospho-p53 (S18) after treatment with purvalanol A. Cells were treated with 1 μM doxorubicin (Doxo) for 4 hr as a positive control.

(E) Western blot for p53 72h after siRNA knockdown of indicated CDKs and cyclins. Ctrl refers to non-targeting control siRNA.

(F) Western blot for p53 in nuclear and cytosolic fractions after 10 μM purvalanol A (purv). Lamin and β-tubulin represent nuclear and cytosolic fractions, respectively.
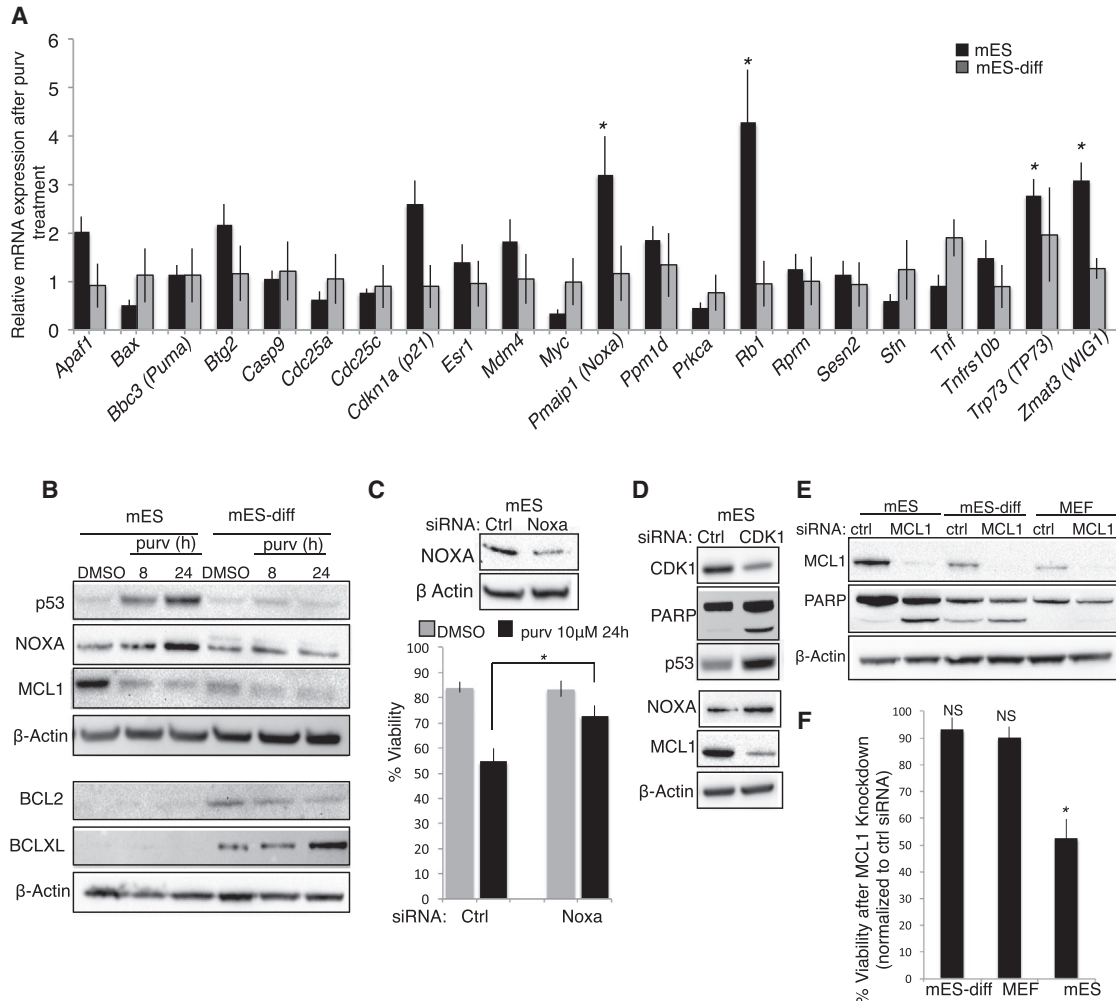
a significant increase in any p53 targets in differentiated cells. These data identify a specific subset of p53 target genes that are upregulated in response to CDK1 inhibition in mESCs.

Of the significantly upregulated p53 targets, RB, TP73, and WIG1 function in cell-cycle arrest and/or p53 stability mechanisms, while only NOXA has a predominantly apoptotic function. NOXA is a BCL2 homology domain 3 (BH3)-only pro-apoptotic member of the BCL2 family of proteins, which regulate cell survival and cell death through the intrinsic apoptotic pathway.

Given the strong connection between NOXA and the intrinsic apoptotic pathway, we chose to investigate whether NOXA mediates CDK1-inhibitor-induced death in mESCs. To verify our array results, we examined mRNA levels of *Bbc3* (PUMA) and *Pmaip1* (NOXA), in response to CDK1 inhibitor treatment by quantitative RT-PCR. Consistent with our array results, we observed no change in *Bbc3* mRNA levels, while *Pmaip1* was significantly upregulated after purvalanol A treatment in mESCs (Figure S3A). Upregulation of *Pmaip1* was not observed in either $p53^{-/-}$ mES or mES-diff cells, indicating that induction of *Pmaip1* is p53-dependent and requires the pluripotent state (Figure S3A). NOXA protein levels also increased upon purvalanol A treatment, which correlated with an increase in p53 protein levels, in mESCs but not mES-diff cells (Figure 5B). Pretreatment of mESCs with NOXA-specific siRNAs prior to purvalanol A treatment significantly reduced the levels of cell death (Figure 5C). These results indicate that NOXA is a major contributor to CDK1-inhibitor-induced cell death in mESCs.

NOXA regulates apoptosis predominately through the inactivation of myeloid cell leukemia sequence 1 (MCL1), an anti-apoptotic BCL2 family member (Deng et al., 2007). Binding of NOXA to MCL1 relieves MCL1's binding and repression of pro-apoptotic proteins and leads to the degradation of MCL1 through the proteasomal pathway (Nakajima et al., 2014). Whether NOXA or MCL1 regulate mouse or human ES cell survival has not been established. Western blot analysis of MCL1 revealed it to be highly expressed in mESCs compared to mES-diff cells (Figure 5B). In contrast, other anti-apoptotic BCL2 family members, BCL2 and BCL-XL, were expressed in mES-diff cells but

Figure 5. CDK1 Inhibition Induces Expression of Bcl2 Family Member NOXA and Depletes MCL1 to Induce Cell Death in mESCs

(A) Fold change mRNA expression of p53 transcriptional targets in mES and mES-diff cells after treatment with purvalanol A for 8 hr (mean ± SEM n = 4 independent experiments). Treated samples were compared to DMSO-treated controls for each cell type. $2(-\Delta ct)$ of treated and untreated populations compared using a Student's t test, *p < 0.05.

(B) Western blot for indicated proteins after 10 μM purvalanol A (purv) treatment for indicated time in hours (h).

(C) Cell viability of mESCs pretreated with siRNA against Noxa after 24-hr treatment with 10 μM purvalanol A (mean ± SEM n = 4 independent experiments). Populations compared using a Student's t test, *p = 0.01. Western blot depicts level of NOXA knockdown achieved at time of purvalanol A treatment.

(D) Western blot analysis of indicated proteins in mESCs after CDK1 siRNA knockdown. Ctrl refers to non-targeting control siRNA.

(E) Western blot analysis of MCL1 and PARP cleavage after siRNA knockdown of MCL1.

(F) Cell viability after siRNA knockdown of MCL1, normalized to a non-targeting control (mean ± SEM n = 4 independent experiments). siRNA-treated and control populations compared by a Student's t tests, *p = 0.0003. NS, not significant.

See also Figure S3

could not be detected in mESCs (Figure 5B), suggesting MCL1 is a predominant regulator of mESC survival. MCL1 protein levels were significantly decreased in mESCs upon purvalanol A treatment, correlating with the increase in NOXA expression (Figure 5B). We confirmed that activation of the p53-NOXA axis and MCL1 depletion was due to CDK1 inhibition, and not an off-target effect of small mole-

cule CDK inhibitors, using siRNA-mediated knockdown of CDK1. Consistent with the small molecule studies, CDK1 depletion resulted in increased protein levels of p53 and NOXA, decreased MCL1, and induction of PARP cleavage (Figure 5D).

We next used siRNAs to deplete MCL1 in mESCs, mESC-diff cells, and MEFs (Figure 5E). MCL1 knockdown

in mESCs resulted in significant levels of cell death (approximately 50%) compared to a non-targeting control (Figures 5E and 5F). While mES-diff cells exhibited low levels of cell death in response to transfection reagents, they did not undergo additional cell death after MCL1 knockdown compared to a non-targeting control (Figures 5E and 5F). MCL1 knockdown also did not induce appreciable cell death in MEFs (Figures 5E and 5F). These results suggest that MCL1 is critical for mESC survival and therefore CDK1 inhibition could selectively kill mESCs though inactivation of MCL1.

hESCs Are Sensitive to CDK1 Inhibition and Express High Levels of MCL1 Compared to Differentiated Cells

Similar to their murine counterparts, hESCs exhibit an accelerated cell-cycle program with a shortened G1 phase, characterized by heightened CDK activity and lack of endogenous CDK inhibitors (Neganova et al., 2009). Despite these similarities, many fundamental differences in cell signaling pathways, including expression patterns of cell-cycle regulatory machinery, have been reported between hESCs and mESCS (Becker et al., 2006; Schnerch et al., 2010). To determine if hESCs are also sensitive to CDK1 inhibition, we treated two independently derived hESC lines, UCSF4 and a Mel1-derived insulin GFP reporter line (Mel1$^{INS/GFP}$) (Micallef et al., 2012), with purvalanol A. Both hESC lines underwent significant cell death after 24 hr of CDK1 inhibitor treatment (Figures 6A and 6B).

We differentiated Mel1$^{INS/GFP}$ hESCs along a pancreatic progenitor lineage using an established 15-day differentiation protocol. Differentiated insulin-producing cells can be readily identified because GFP is expressed from the insulin promoter. This protocol generates a hESC-derived pancreatic progenitor cell population with an average of ∼5% insulin-producing cells (Guo et al., 2013; Schulz et al., 2012). We did not observe significant cell death when differentiated Mel1$^{INS/GFP}$ hESCs were treated with purvalanol A (Figures 6A and 6B). Both undifferentiated and differentiated Mel1$^{INS/GFP}$ hESCs arrested in G2/M to a similar extent after purvalanol A treatment, indicating that CDK1 was being targeted in both cell types (Figure 6C). Furthermore, we did not see a significant change in the percentage of insulin-expressing cells, by fluorescence-activated cell sorting (FACS) analysis of GFP expression (Figure 6D), indicating that CDK1 inhibitor treatment does not affect the differentiated insulin-producing population of cells. Thus, CDK1 inhibition elicits cell death in both mouse and human undifferentiated ESCs but not cells that have been differentiated, supporting a common dependency on CDK1 in mouse and human ESCs.

To determine whether CDK1 inhibition induces cell death in hESCs and mESCs through similar mechanisms, we assessed protein levels of γ-H2AX and p53 after CDK1 inhibitor treatment in hESCs. 24-hr treatment with purvalanol A resulted in increased levels of γ-H2AX in undifferentiated but not differentiated hESCs (Figure 6B). p53 expression levels were also increased in hESCs after purvalanol A treatment (Figure 6B). The increase in p53 protein was accompanied by a significant increase in expression of NOXA, both at the mRNA (Figure 6E) and protein level (Figure 6F). Interestingly, differentiated hESCs also exhibited an increase in p53 levels after purvalanol A treatment, without appreciable cell death (Figure 6B). We did not, however, observe an increase in NOXA mRNA or protein levels in differentiated hESCs, despite the increased p53 expression (Figures 6E and 6F). Thus, CDK1 inhibition in differentiated hESCs results in increased p53 expression, without downstream activation of NOXA or subsequent cell death.

Increased NOXA expression in hESCs after purvalanol A treatment implicates a change in MCL1 activity as a mediator of CDK1-inhibitor-induced death. Western blot analysis revealed that, similar to mESCs, MCL1 is highly expressed in hESCs compared to differentiated hESCs (Figure 6F). Other anti-apoptotic family members, BCL2 and BCL-XL, were expressed at lower levels in hESCs compared to differentiated hESCs (Figure 6F), indicating MCL1 as a predominant anti-apoptotic factor expressed in hESCs. To determine whether CDK1 inhibition induced cell death in hESCs through altered MCL1 expression, we examined total MCL1 protein levels after treatment with purvalanol A. In contrast to mESCs, we did not see a significant decrease in total MCL1 levels in hESCs after purvalanol A treatment (Figure 6F). NOXA can block MCL1's ability to inhibit the pro-apoptotic function of BAX and BAK without markedly changing MCL1's abundance (Hauck et al., 2009). Thus, increased NOXA expression in the presence of even a modest decrease of MCL1 expression would be expected to sensitize hESCs for cell death.

In addition to inhibition by NOXA, MCL1 is also regulated by phosphorylation by multiple kinases known to regulate both its stability and activity (Hauck et al., 2009). CDK1 has been shown to directly phosphorylate serine 64 (S64) of human, but not mouse, MCL1 (Kobayashi et al., 2007). Mouse MCL1 contains a glutamic acid rather than a serine at this residue, which likely functions as a constitutive phosphomimetic. Phosphorylation of S64 by CDK1 enhances its anti-apoptotic function of MCL1 without affecting protein stability (Kobayashi et al., 2007). Purvalanol A treatment resulted in a decrease in S64 phosphorylation of MCL1 (Figure 6F). These data suggest that CDK1 inhibition negatively affects the anti-apoptotic function of MCL1 in hESCs, both indirectly through induction of NOXA and directly through loss of phosphorylation of S64. Furthermore, siRNA knockdown of MCL1 induced cell death in H9 hESCs, but not human
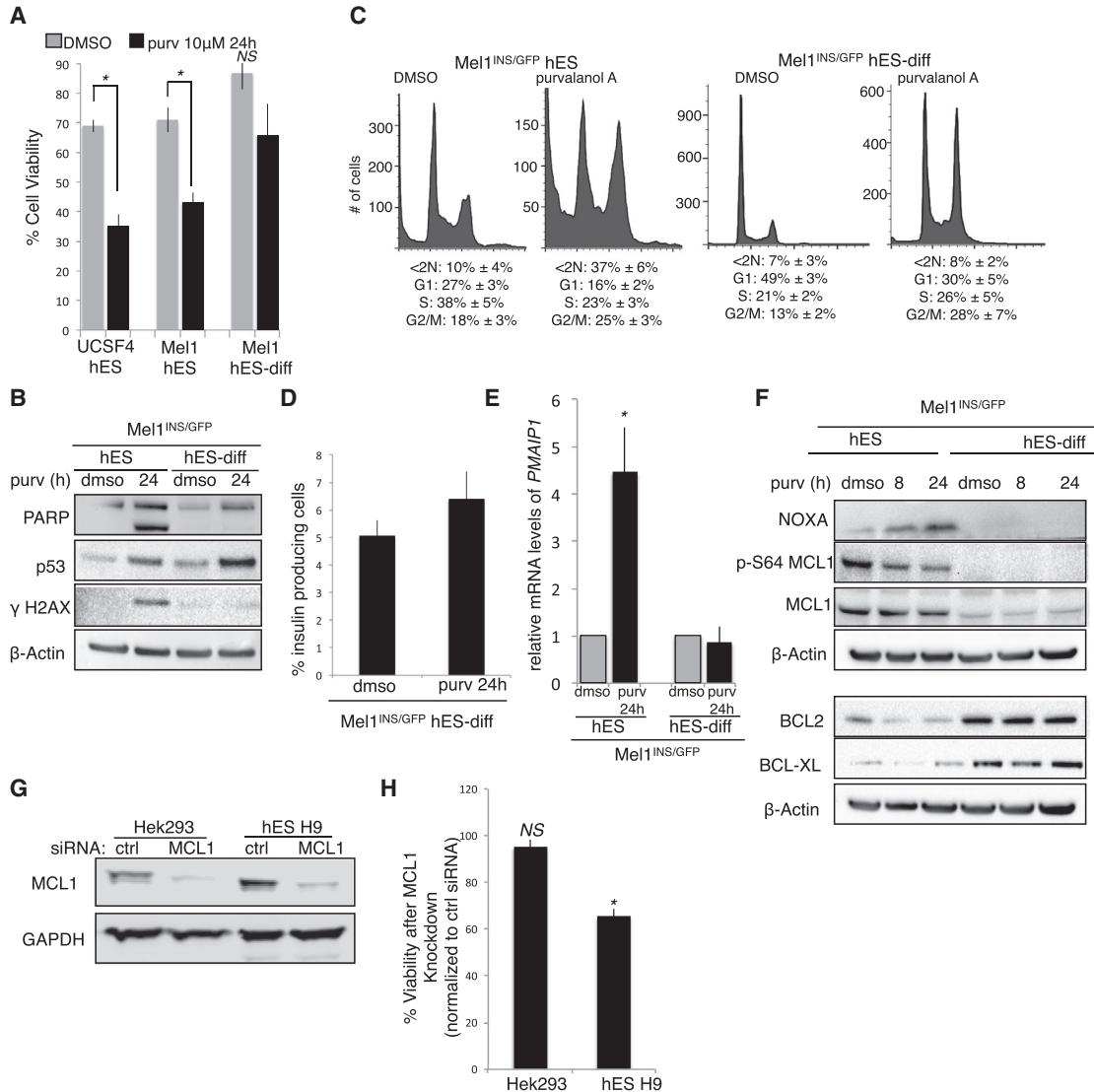
Figure 6. Small Molecule Inhibition of CDK1 Induces Apoptosis in hESCs

(A) Cell viability after 24-hr treatment with DMSO or purvalanol A (10 μM) (mean ± SEM n = 3 independent experiments). Populations were compared using a Student's t test *p < 0.01. NS, not significant.

(B) Western blot analysis of indicated proteins in hESCs and differentiated hESCs (hESC-diff) after purvalanol A treatment for 24 hr.

(C) Effect of purvalanol A on undifferentiated and differentiated hES cell cycle distribution. Percentages of cells in each cell-cycle phase, mean ± SEM, n = 3 independent experiments.

(D) Percentage of insulin-producing cells as determined with FACS analysis using an insulin-GFP reporter cell line (mean ± SEM n = four independent experiments).

(E) Relative expression of *PMAIP1* mRNA after purvalanol A treatment in hESCs and hESC-diff, determined by quantitative PCR (mean ± SEM n = four independent experiments). Treated samples compared to untreated samples for each cell type independently, using a paired Student's t test, *p < 0.05.

(F) Western blot analysis of indicated proteins after purvalanol A treatment for indicated time in hours (h).

(G) Western blot analysis of MCL1 after siRNA knockdown of MCL1.

(H) Cell viability after siRNA knockdown of MCL1, normalized to a non-targeting control (mean ± SEM n = 4 independent experiments). siRNA-treated and control populations compared by a Student's t tests, *p = 0.02. NS, not significant.

embryonic kidney (HEK293) cells, a differentiated cell type (Figures 6G and 6H), suggesting that MCL1 is critical for hESC survival. It has recently been shown that hESCs are highly primed toward apoptosis due to the balance of pro- and anti-apoptotic proteins, particularly the low expression of BCL2 (Liu et al., 2013). Our present work adds to this hypothesis and suggests MCL1 is a critical regulator of hESC survival. We therefore conclude that high MCL1 expression sensitizes hESCs to MCL1 deregulation, and CDK1 inhibition induces apoptosis in hESCs by negatively regulating MCL1 anti-apoptotic function.

CDK1 Inhibition Depletes OCT4-Positive Undifferentiated Cells and Prevents the Growth of Stem Cell-Derived Tumors

Our data suggest that pluripotent cells are uniquely sensitive to CDK1 inhibition. We reasoned that CDK1 inhibitors could selectively deplete residual undifferentiated cells during stem cell transplantation, thus reducing the occurrence of ESC-derived teratomas. We generated a partially differentiated ESC population by treating mESCs with RA for 2 days, resulting in greater than 80% reduction of *Oct4* mRNA expression (Figure S2A). Immunofluorescence analysis revealed a heterogeneous population of cells based on the expression patterns of OCT4 and Nanog (Figure 7A). Treatment of partially differentiated mESC populations with 15 μM purvalanol A for 24 hr significantly reduced the percentage of OCT4 and Nanog-expressing cells (Figures 7A and 7B). These results indicate that CDK1 inhibition preferentially depletes pluripotent cells within a partially differentiated population.

To determine if depletion of OCT4 and Nanog-expressing cells would reduce the risk of teratoma formation, we subcutaneously transplanted into BALB/c Nu/Nu mice with equal numbers of viable, partially differentiated mESCs, treated with either 15 μM purvalanol A or DMSO for 24 hr, and monitored daily for tumor formation. Transplants with DMSO-treated cells resulted in visible tumors as early as 5 days after transplantation, with 17 of 18 mice developing tumors during the 45-day course of the experiment (Figure 7C). Mice transplanted with purvalanol-A-treated cells exhibited decreased tumor incidence, with only 3 of 13 mice developing visible tumors (Figure 7C), suggesting that CDK1 inhibition depletes tumorigenic cells from a heterogeneous population.

We next investigated if in vivo treatment with CDK inhibitors could prevent the formation of stem cell-derived tumors. We used an alternative CDK inhibitor, dinaciclib, which has improved pharmacokinetic properties compared to purvalanol A (Parry et al., 2010). Dinaciclib inhibits CDK1, 2, 5, and 9 and is currently in clinical trials against multiple tumor types (Dickson and Schwartz, 2009). Mice were transplanted with viable, partially differ-entiated mESCs and treated with intraperitoneal (i.p.) injections of dinaciclib or diluent control starting 72 hr after transplant. A treatment regimen of twice-weekly intraperitoneal injections was continued for 4 weeks. Mice in the control group developed tumors as early as 5 days post-transplantation, with four of five mice developing tumors over the course of the 4-week experiment (Figure 7D). In contrast only one out of seven of the dinaciclib-treated mice developed a tumor (Figure 7D). Therefore, in vivo treatment with a CDK1 inhibitor decreases the formation of stem cell-derived tumors.

Tumors that formed after transplantation with partially differentiated mESCs grew aggressively, reaching the ethical endpoint (400 mm^2) within 2–3 weeks after detection. We asked if dinaciclib treatment would attenuate the growth of established stem cell-derived tumors. We transplanted mice with partially differentiated mESCs and allowed tumors to develop. When palpable tumors formed (range, 50–100 mm^2 in volume), we began intraperitoneal injections with dinaciclib or diluent control. Within the control group, tumors continued to grow rapidly, reaching the ethical endpoint within 2 weeks after injections began. Dinaciclib-treated mice tumors grew significantly more slowly, indicating that CDK inhibitors slow the growth of established stem cell-derived tumors (Figures 7E and 7F).

The difference in growth rate of treated versus untreated cells led us to ask if dinaciclib treatment affected tumor composition. At the end of the 26-day treatment regimen or when tumors reached the ethical size endpoint, we collected tumors and stained with hematoxylin and eosin (H&E). In a blinded analysis, ten fields from each tumor were characterized based on their percentage composition of the following categories: necrosis, embryonal carcinoma, immature teratoma (including primitive epithelium/neuroepithelium and cellular atypical glial tissue), mature teratoma (including respiratory epithelium, squamous epithelium, and cartilage), and other (including inflammatory cells and stromal tissue). Tumors from the control group exhibited tissues derived from all three germ layers and showed substantial components of embryonal carcinoma and immature teratoma (Figure S4). There was a decrease in the immature teratoma component after dinaciclib treatment (Figure 7G; Figure S4). Furthermore, tumors from the dinaciclib-treated group showed an increase in necrotic tissue (Figure 7G; Figure S4A), suggesting that some stem cell-derived tissues were undergoing cell death after dinaciclib treatment. Because dinaciclib targets CDKs 2, 5, and 9 in addition to CDK1, we asked if off-target effects might contribute to stem cell death. We previously showed that siRNA knockdown of CDK2 has no effect on mESC viability (Figure 1C). We found that siRNA knockdown of CDKs 5 and 9 also had no effect on cell cycle or
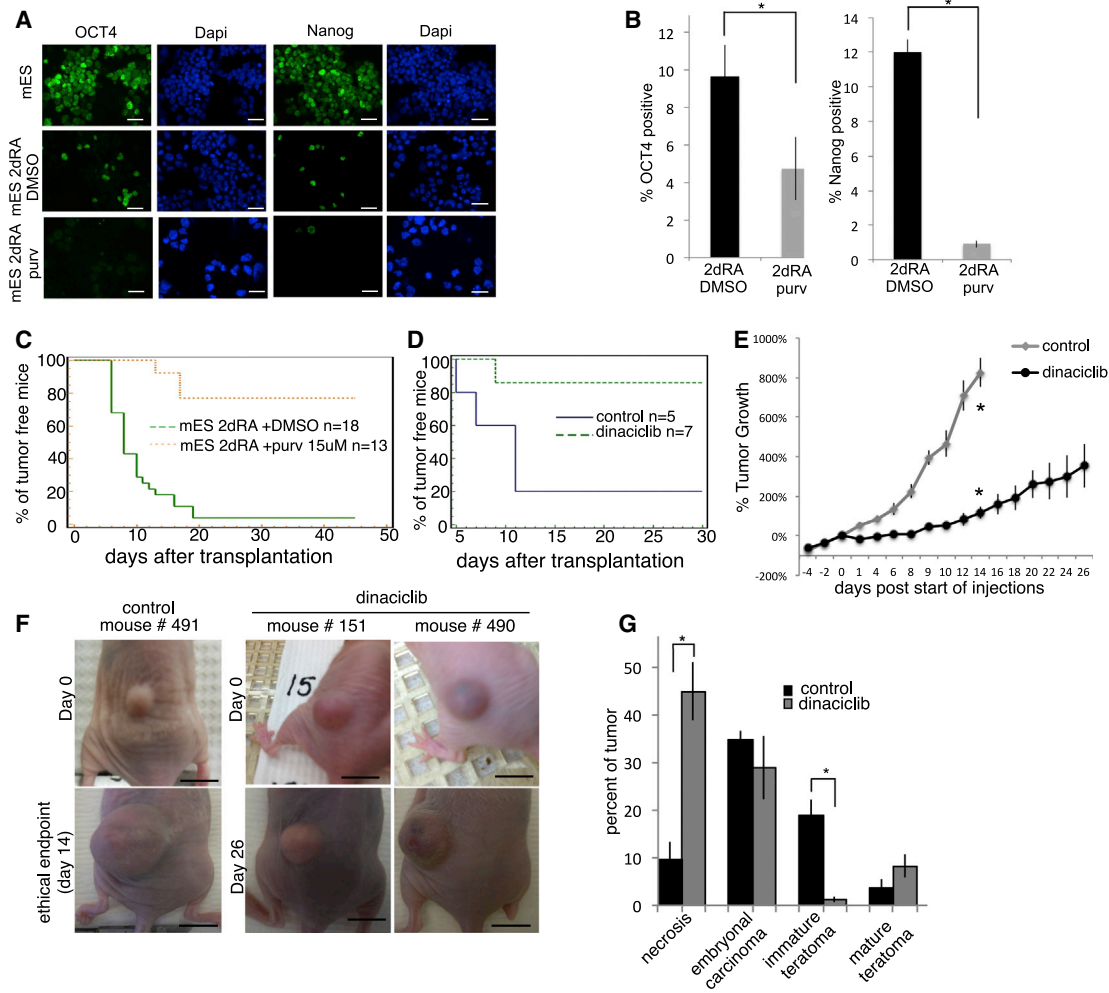
Figure 7. Treatment with CDK1 Inhibitors Prevents mESC-Driven Tumors In Vivo

(A) OCT4 and Nanog expression in undifferentiated mESCs and after 2 days of treatment with 1 μM retinoic acid (mES 2dRA) ± 15 μm purvalanol A for 24 hr. Scale bar, 40 μm (left).

(B) Percentage of OCT4-positive (left) and Nanog-positive (right) cells from immunofluorescence experiment in (A) (mean ± SEM n = 3 independent experiments). Populations compared using a Student's t test, *p < 0.02.

(C) Kaplan-Meier graph showing the percentage of mice that remained teratoma free after subcutaneous transplantation. Significance of differences in each population determined by the log rank test, p = 0.001.

(D) Kaplan-Meier graph showing the percentage of mice that remained teratoma free after subcutaneous transplantation with partially differentiated ES cells. Mice received dinaciclib or vehicle treatment. p < 0.05, determined by the log rank test.

(E) Percentage tumor growth in mice injected with dinaciclib (n = 7) versus vehicle (n = 8). Control and treated mice after 14 days of treatment compared using a Student's t test *p = 0.0001.

(F) Mouse teratomas after treatment with dinaciclib or vehicle. Scale bars, 10 mm.

(G) Quantification of tumor composition, based on defined categories. Control- (n = 8) and dinaciclib-treated tumors (n = 7) compared using a Student's t test, *p < 0.0004.

See also Figure S4.

cell viability of mES cells (Figures S4B and S4C). These results raise the intriguing possibility that CDK1 inhibition in vivo attenuates tumor growth by selectively killing poorly differentiated, immature stem cell-derived tumor components.

DISCUSSION

In this study, we investigate the unique cell-cycle dependencies of mouse and human ES cells. We discovered that inhibition or depletion of CDK1 or its associated cyclins

can selectively cause DNA damage and induce apoptosis in ESCs. In contrast, inhibition or depletion of other cyclins or CDKs in ESCs failed to induce appreciable cell death. We find that mouse and human ESCs exhibit increased p53 activity, NOXA induction, MCL1 inactivation, and subsequent cell death after CDK1 inhibition. Furthermore, we show that CDK1 inhibitors can prevent mESC-derived tumors and inhibit the growth of established tumors. These results demonstrate a unique requirement for CDK1 in mouse and human ES cells and identify CDK1 as a potential therapeutic target to prevent or treat stem cell-derived tumors.

Our findings indicate that the G2/M/G1 transition events that are regulated by CDK1 activity are the most critical for the proliferation and survival of ESCs. Depletion of cyclin D1 or E cyclins and CDK2 did not have appreciable effects on cell proliferation and did not induce cell death (Figure 1). These results are consistent with the observation that loss of CDK4/6 or CDK2 can be compensated by CDK1 activity (Santamaría et al., 2007). CDK1 activity, however, is also critically important for overall genome stability, including the maintenance of faithful chromosome segregation and the ability of cellular DNA damage repair to occur through homologous recombination (Johnson et al., 2011; Keeney and Neale, 2006; Peterson et al., 2011). Thus, the unique dependency of ESCs on CDK1 activity may ensure that cells that have failed appropriate transitions in G2/M/G1, and are therefore at risk for harboring aberrant genomes, will be eliminated through apoptosis.

A secondary mechanism to ensure genomic fidelity is manifested in a switch in the apoptotic program employed by ESCs. In this study, we discovered a cell-death pathway involving NOXA and MCL1 that is uniquely activated to induce cell death in ESC but not differentiated cells. The apoptotic potential of NOXA overexpression is dependent on the cellular and genetic context (Ploner et al., 2008). Compared to other BH3-only proteins, including PUMA, BIM, or BAD, NOXA exhibits the most limited potential to bind and sequester anti-apoptotic proteins, binding almost exclusively to MCL1 (Chen et al., 2005). Therefore, susceptibility to NOXA-induced cell death is dependent on MCL1 activity relative to other anti-apoptotic proteins (Ploner et al., 2008). We find that mouse and human ESCs highly express MCL1, but not other anti-apoptotic proteins, such as BCL2 or BCL-XL. In contrast, upon differentiation MCL1 expression decreases, but BCL2 and BCL-XL expression is induced. Thus, an apparent "apoptotic switch" occurs as cells transition from pluripotency to a differentiated state. Consistent with this observation, we find that both mouse and human ESCs, but not diff-ESCs are sensitive to MCL1 inhibition (Figures 5 and 7). CDK1 inhibition acts at multiple steps to inactivate MCL1, both by inducing NOXA, as well as through inhibition of S64 phosphorylation in hESCs.

A recent study by Liu et al. (2013) demonstrated that the mitochondria of hESCs are highly primed to undergo DNA damage-induced apoptosis. Our current study has identified a unique upstream stimulus via CDK1 inhibition that selectively induces DNA damage in ESCs but not appreciably in differentiated cells. Taken together, the emerging picture is one where ESCs, upon inactivation of CDK1, experience DNA damage that differentiated cells do not perceive and are also poised to die in response to this damage.

In this study, we exploit the unique cell cycle of mouse and human ES cells to induce selective cell killing. We found that the CDK1 inhibitor purvalanol A effectively depleted the Nanog and OCT4-expressing cells from a mixed population of differentiated and undifferentiated cells. Furthermore, we show that a clinically relevant CDK inhibitor, dinaciclib, can both prevent the initiation and inhibit the progression of stem cell-driven tumors in vivo. Our study identifies critical differences in the pathways controlling cellular proliferation and apoptosis of ESCs versus differentiated cells. ESCs are poised to utilize a p53-NOXA-MCL1 axis to respond to DNA damage induced by CDK1 inhibition and undergo cell death.

EXPERIMENTAL PROCEDURES

Cell Culture

Mouse embryonic stem cell lines, E14, oct4-GFP E14, p1.2 (p53$^{-/-}$), DGCR8$^{-/-}$, and Bax$^{-/-}$ Bak$^{-/-}$ were maintained on plates coated with 0.2% gelatin in knockout DMEM (Gibco) supplemented with 15% FBS, 1 × nonessential amino acids, 1 × glutaMAX-1, 100 units/ml penicillin-streptomycin, and 0.1 μM 2-mercaptoethanol and recombinant leukemia inhibitory factor. miPS cells were generated as previously described (Takahashi and Yamanaka, 2006). UCSF4 (NIH registry no. is 0044) and Mel1$^{INS/GFP}$ (Micallef et al., 2012) human embryonic stem cells were maintained on non-proliferative MEFs in standard DMEM/F12 medium supplemented with 10 ng/ml FGF2. MEFs and HEK293 cells were grown in DMEM supplemented with 10% FBS and 100 units/ml penicillin-streptomycin. H9 human embryonic stem cells were maintained on matrigel coated plates in Essential 8 media (Gibco). All cell lines were maintained in 5% CO2 at 37°C. mESCs were reverse-transfected, and hESCs were forward-transfected, using Lipofectamine RNAi MAX (Invitrogen), according to manufacturers instructions. siRNAs and a pool of non-targeting control siRNA (Dharmacon control #2) were purchased from Dharmacon (siGENOME SMART pool siRNA; Dharmacon) and used at a concentration of 50 nM (cyclins, Noxa and Mcl1) or 100 nM (Cdks). All human ES cell line experiments were approved by the University of California San Francisco institutional use committee.

Protein Preparation and Western Blotting

Cultured cells were harvested into radioimmunoprecipitation assay (RIPA) buffer (50 mM Tris, 150 mM NaCl, 0.5%

sodium-deoxycholate, 1% NP-40, 0.1% SDS, 2 mM EDTA [pH 7.5]) containing COMPLETE protease inhibitor cocktail (Roche) and phosphatase inhibitors (Santa Cruz Biotechnology). Protein concentrations were determined by performing DC Protein Assay (Bio-Rad) using BSA as standard. See Supplemental Information for antibodies used.

Cell-Cycle and Cell-Death Analysis

Cell viability was determined using a flow-cytometry-based Guava ViaCount viability assay (Millipore), performed according to the manufacturer's instruction. For cell-cycle analysis, cells were fixed by dropwise addition of ice-cold EtOH and storage at −20C. Fixed cells were stained with propidium iodide, and samples were analyzed on a LSRII flow cytometer (BD Biosciences). Cell populations were gated to exclude doublets. Sub2N levels were determined using FlowJo (Tree Star) analysis software. Univariate cell-cycle analysis was performed by excluding dead cells and using the Watson model cell-cycle analysis program provided by FlowJo analysis software.

EC_{50} Calculations

The half-maximal response (EC_{50}) was estimated by nonlinear regression analysis of the concentration-response curves using GraphPad Prism. Response presented as percentage maximal response for each cell type. Fisher's exact test was used to determine the significance of differences in EC_{50} values for each cell type.

Mouse Xenograft Studies

All animal experiments were approved by the University of California San Francisco institutional animal care and use committee. For complete description of xenograft studies and all other additional methods, please see Supplemental Information.

SUPPLEMENTAL INFORMATION

Supplemental Information includes Supplemental Experimental Procedures and four figures and can be found with this article online at http://dx.doi.org/10.1016/j.stemcr.2015.01.019.

REFERENCES

Ballabeni, A., Park, I.H., Zhao, R., Wang, W., Lerou, P.H., Daley, G.Q., and Kirschner, M.W. (2011). Cell cycle adaptations of embryonic stem cells. Proc. Natl. Acad. Sci. USA 108, 19252–19257.

Barrière, C., Santamaría, D., Cerqueira, A., Galán, J., Martín, A., Ortega, S., Malumbres, M., Dubus, P., and Barbacid, M. (2007). Mice thrive without Cdk4 and Cdk2. Mol. Oncol. 1, 72–83.

Becker, K.A., Ghule, P.N., Therrien, J.A., Lian, J.B., Stein, J.L., van Wijnen, A.J., and Stein, G.S. (2006). Self-renewal of human embryonic stem cells is supported by a shortened G1 cell cycle phase. J. Cell. Physiol. 209, 883–893.

Brooks, E.E., Gray, N.S., Joly, A., Kerwar, S.S., Lum, R., Mackman, R.L., Norman, T.C., Rosete, J., Rowe, M., Schow, S.R., et al. (1997). CVT-313, a specific and potent inhibitor of CDK2 that prevents neointimal proliferation. J. Biol. Chem. 272, 29207–29211.

Canman, C.E., Lim, D.S., Cimprich, K.A., Taya, Y., Tamai, K., Sakaguchi, K., Appella, E., Kastan, M.B., and Siliciano, J.D. (1998). Activation of the ATM kinase by ionizing radiation and phosphorylation of p53. Science 281, 1677–1679.

Chen, L., Willis, S.N., Wei, A., Smith, B.J., Fletcher, J.I., Hinds, M.G., Colman, P.M., Day, C.L., Adams, J.M., and Huang, D.C. (2005). Differential targeting of prosurvival Bcl-2 proteins by their BH3-only ligands allows complementary apoptotic function. Mol. Cell 17, 393–403.

Deng, J., Carlson, N., Takeyama, K., Dal Cin, P., Shipp, M., and Letai, A. (2007). BH3 profiling identifies three distinct classes of apoptotic blocks to predict response to ABT-737 and conventional chemotherapeutic agents. Cancer Cell 12, 171–185.

Dickson, M.A., and Schwartz, G.K. (2009). Development of cell-cycle inhibitors for cancer therapy. Curr. Oncol. 16, 36–43.

Falck, J., Forment, J.V., Coates, J., Mistrik, M., Lukas, J., Bartek, J., and Jackson, S.P. (2012). CDK targeting of NBS1 promotes DNA-end resection, replication restart and homologous recombination. EMBO Rep. 13, 561–568.

Goga, A., Yang, D., Tward, A.D., Morgan, D.O., and Bishop, J.M. (2007). Inhibition of CDK1 as a potential therapy for tumors over-expressing MYC. Nat. Med. 13, 820–827.

Gray, N.S., Wodicka, L., Thunnissen, A.M., Norman, T.C., Kwon, S., Espinoza, F.H., Morgan, D.O., Barnes, G., LeClerc, S., Meijer, L., et al. (1998). Exploiting chemical libraries, structure, and genomics in the search for kinase inhibitors. Science 281, 533–538.

Guo, T., Landsman, L., Li, N., and Hebrok, M. (2013). Factors expressed by murine embryonic pancreatic mesenchyme enhance generation of insulin-producing cells from hESCs. Diabetes 62, 1581–1592.

Hauck, P., Chao, B.H., Litz, J., and Krystal, G.W. (2009). Alterations in the Noxa/Mcl-1 axis determine sensitivity of small cell lung cancer to the BH3 mimetic ABT-737. Mol. Cancer Ther. 8, 883–892.

Horiuchi, D., Huskey, N.E., Kusdra, L., Wohlbold, L., Merrick, K.A., Zhang, C., Creasman, K.J., Shokat, K.M., Fisher, R.P., and Goga, A. (2012). Chemical-genetic analysis of cyclin dependent kinase 2 function reveals an important role in cellular transformation by multiple oncogenic pathways. Proc. Natl. Acad. Sci. USA 109, E1019–E1027.

Johnson, N., Li, Y.C., Walton, Z.E., Cheng, K.A., Li, D., Rodig, S.J., Moreau, L.A., Unitt, C., Bronson, R.T., Thomas, H.D., et al. (2011). Compromised CDK1 activity sensitizes BRCA-proficient cancers to PARP inhibition. Nat. Med. 17, 875–882.

Kalaszczynska, I., Geng, Y., Iino, T., Mizuno, S., Choi, Y., Kondratiuk, I., Silver, D.P., Wolgemuth, D.J., Akashi, K., and Sicinski, P. (2009). Cyclin A is redundant in fibroblasts but essential in hematopoietic and embryonic stem cells. Cell 138, 352–365.

Keeney, S., and Neale, M.J. (2006). Initiation of meiotic recombination by formation of DNA double-strand breaks: mechanism and regulation. Biochem. Soc. Trans. 34, 523–525.

Kobayashi, S., Lee, S.H., Meng, X.W., Mott, J.L., Bronk, S.F., Werneburg, N.W., Craig, R.W., Kaufmann, S.H., and Gores, G.J. (2007). Serine 64 phosphorylation enhances the antiapoptotic function of Mcl-1. J. Biol. Chem. 282, 18407–18417.

Li, V.C., Ballabeni, A., and Kirschner, M.W. (2012). Gap 1 phase length and mouse embryonic stem cell self-renewal. Proc. Natl. Acad. Sci. USA 109, 12550–12555.

Liu, J.C., Guan, X., Ryan, J.A., Rivera, A.G., Mock, C., Agrawal, V., Letai, A., Lerou, P.H., and Lahav, G. (2013). High mitochondrial priming sensitizes hESCs to DNA-damage-induced apoptosis. Cell Stem Cell 13, 483–491, Erratum in Cell Stem Cell. 2013;13:634. Agarwal, Vishesh [corrected to Agrawal, Vishesh].

Micallef, S.J., Li, X., Schiesser, J.V., Hirst, C.E., Yu, Q.C., Lim, S.M., Nostro, M.C., Elliott, D.A., Sarangi, F., Harrison, L.C., et al. (2012). INS(GFP/w) human embryonic stem cells facilitate isolation of in vitro derived insulin-producing cells. Diabetologia 55, 694–706.

Momcilovic, O., Knobloch, L., Fornsaglio, J., Varum, S., Easley, C., and Schatten, G. (2010). DNA damage responses in human induced pluripotent stem cells and embryonic stem cells. PLoS ONE 5, e13410.

Morgan, D.O. (2007). The Cell Cycle: Principles of Control (New Science Press).

Nakajima, W., Hicks, M.A., Tanaka, N., Krystal, G.W., and Harada, H. (2014). Noxa determines localization and stability of MCL-1 and consequently ABT-737 sensitivity in small cell lung cancer. Cell Death Dis. 5, e1052.

Neganova, I., Zhang, X., Atkinson, S., and Lako, M. (2009). Expression and functional analysis of G1 to S regulatory components reveals an important role for CDK2 in cell cycle regulation in human embryonic stem cells. Oncogene 28, 20–30.

Orford, K.W., and Scadden, D.T. (2008). Deconstructing stem cell self-renewal: genetic insights into cell-cycle regulation. Nat. Rev. Genet. 9, 115–128.

Parry, D., Guzi, T., Shanahan, F., Davis, N., Prabhavalkar, D., Wiswell, D., Seghezzi, W., Paruch, K., Dwyer, M.P., Doll, R., et al. (2010). Dinaciclib (SCH 727965), a novel and potent cyclin-dependent kinase inhibitor. Mol. Cancer Ther. 9, 2344–2353.

Peterson, S.E., Li, Y., Chait, B.T., Gottesman, M.E., Baer, R., and Gautier, J. (2011). Cdk1 uncouples CtIP-dependent resection and Rad51 filament formation during M-phase double-strand break repair. J. Cell Biol. 194, 705–720.

Ploner, C., Kofler, R., and Villunger, A. (2008). Noxa: at the tip of the balance between life and death. Oncogene 27 (Suppl 1), S84–S92.

Sabapathy, K., Klemm, M., Jaenisch, R., and Wagner, E.F. (1997). Regulation of ES cell differentiation by functional and conformational modulation of p53. EMBO J. 16, 6217–6229.

Santamaría, D., Barrière, C., Cerqueira, A., Hunt, S., Tardy, C., Newton, K., Cáceres, J.F., Dubus, P., Malumbres, M., and Barbacid, M. (2007). Cdk1 is sufficient to drive the mammalian cell cycle. Nature 448, 811–815.

Schnerch, A., Cerdan, C., and Bhatia, M. (2010). Distinguishing between mouse and human pluripotent stem cell regulation: the best laid plans of mice and men. Stem Cells 28, 419–430.

Schulz, T.C., Young, H.Y., Agulnick, A.D., Babin, M.J., Baetge, E.E., Bang, A.G., Bhoumik, A., Cepa, I., Cesario, R.M., Haakmeester, C., et al. (2012). A scalable system for production of functional pancreatic progenitors from human embryonic stem cells. PLoS ONE 7, e37004.

Shiloh, Y. (2003). ATM and related protein kinases: safeguarding genome integrity. Nat. Rev. Cancer 3, 155–168.

Stead, E., White, J., Faast, R., Conn, S., Goldstone, S., Rathjen, J., Dhingra, U., Rathjen, P., Walker, D., and Dalton, S. (2002). Pluripotent cell division cycles are driven by ectopic Cdk2, cyclin A/E and E2F activities. Oncogene 21, 8320–8333.

Takahashi, K., and Yamanaka, S. (2006). Induction of pluripotent stem cells from mouse embryonic and adult fibroblast cultures by defined factors. Cell 126, 663–676.

Takeuchi, O., Fisher, J., Suh, H., Harada, H., Malynn, B.A., and Korsmeyer, S.J. (2005). Essential role of BAX,BAK in B cell homeostasis and prevention of autoimmune disease. Proc. Natl. Acad. Sci. USA 102, 11272–11277.

Tetsu, O., and McCormick, F. (2003). Proliferation of cancer cells despite CDK2 inhibition. Cancer Cell 3, 233–245.

Ullah, Z., Kohn, M.J., Yagi, R., Vassilev, L.T., and DePamphilis, M.L. (2008). Differentiation of trophoblast stem cells into giant cells is triggered by p57/Kip2 inhibition of CDK1 activity. Genes Dev. 22, 3024–3036.

van den Heuvel, S., and Harlow, E. (1993). Distinct roles for cyclin-dependent kinases in cell cycle control. Science 262, 2050–2054.

Vassilev, L.T., Tovar, C., Chen, S., Knezevic, D., Zhao, X., Sun, H., Heimbrook, D.C., and Chen, L. (2006). Selective small-molecule inhibitor reveals critical mitotic functions of human CDK1. Proc. Natl. Acad. Sci. USA 103, 10660–10665.

Vousden, K.H., and Lu, X. (2002). Live or let die: the cell's response to p53. Nat. Rev. Cancer 2, 594–604.

Wang, Y., Medvid, R., Melton, C., Jaenisch, R., and Blelloch, R. (2007). DGCR8 is essential for microRNA biogenesis and silencing of embryonic stem cell self-renewal. Nat. Genet. 39, 380–385.

Wei, M.C., Zong, W.X., Cheng, E.H., Lindsten, T., Panoutsakopou-lou, V., Ross, A.J., Roth, K.A., MacGregor, G.R., Thompson, C.B., and Korsmeyer, S.J. (2001). Proapoptotic BAX and BAK: a requisite gateway to mitochondrial dysfunction and death. Science 292, 727–730.

Zhang, Y., and Xiong, Y. (2001). A p53 amino-terminal nuclear export signal inhibited by DNA damage-induced phosphorylation. Science 292, 1910–1915.